Available online at www.sciencedirect.com
SCIENCE DIRECT
C. R. Physique 6 (2005) 33–46
COMPTES RENDUS PHYSIQUE
http://france.elsevier.com/direct/COMREN/

Self-organization on surfaces/Auto-organisation sur les surfaces

Self-organized epitaxial growth on spontaneously nano-patterned templates

Sylvie Rousset [a,*] Bernard Croset [b], Yann Girard [a], Geoffroy Prévot [b], Vincent Repain [a], Stanislas Rohart [a]

[a] *Matériaux et phénoménes quantiques, université Paris 7, CNRS, case 7021, 2, place Jussieu, 75005 Paris, France*
[b] *Groupe de physique des solides, universités Paris 6 et Paris 7, CNRS, campus de Boucicaut, 140, rue de Lourmel, 75015 Paris, France*

Available online 12 January 2005

Presented by Guy Laval

Abstract

Self-ordering at crystal surfaces has been the subject of intense efforts during the last ten years, since it has been recognized as a promising way for growing uniform nanostructures with regular sizes and spacings in the 1–100 nm range. In this article we give an overview of the self-organized nanostructures growth on spontaneously nano-patterned templates. A great variety of surfaces exhibits a nano-scale order at thermal equilibrium, including adsorbate-induced reconstruction, surface dislocations networks, vicinal surfaces or more complex systems. Continuum models have been proposed where long-range elastic interactions are responsible for spontaneous periodic domain formation. Today the comparison between experiments such as Grazing Incidence X-Ray Diffraction experiments and calculations has lead to a great improvement of our fundamental understanding of the physics of self-ordering at crystal surfaces. Then, epitaxial growth on self-ordered surfaces leads to nanostructures organized growth. The present knowledge of modelization of such an heterogeneous growth using multi-scaled calculations is discussed. Such a high quality of both long-range and local ordered growth opens up the possibility of making measurements of physical properties of such nanostructures by macroscopic integration techniques. ***To cite this article: S. Rousset et al., C. R. Physique 6 (2005).***

Résumé

Nucléation et croissance de nanostructures ordonnées sur des surfaces auto-organisées. Depuis une dizaine d'années, la découverte des phénomènes d'auto-organisation à la surface des cristaux a suscité un engouement croissant. La force motrice de ce phénomène est une interaction élastique à longue portée due aux contraintes intrinsèques des surfaces. Ce phénomène « naturel » permet d'élaborer toute une gamme de substrats pré-structurés de 1 à 100 nm, qui servent ensuite de guide à la croissance des nanostructures. L'objectif premier de cette croissance organisée par rapport à la croissance aléatoire est la réalisation de nanostructures dont la dispersion en taille est étroite. Ceci ouvre la voie aux études des propriétés individuelles et collectives de ces nano-objets par des techniques macroscopiques faisant des moyennes sur un grand nombre d'objets (mesures optiques, électroniques ou magnétiques). ***Pour citer cet article : S. Rousset et al., C. R. Physique 6 (2005).***

* Corresponding author.
E-mail addresses: rousset@gps.jussieu.fr (S. Rousset), croset@gps.jussieu.fr (B. Croset), ygirard@gps.jussieu.fr (Y. Girard), prevot@gps.jussieu.fr (G. Prévot), repain@gps.jussieu.fr (V. Repain), rohart@gps.jussieu.fr (S. Rohart).

1631-0705/$ – see front matter
doi:10.1016/j.crhy.2004.11.010

Keywords: Metal surfaces; Self-ordering; Nanostructures growth

Mots-clés : Surfaces métalliques ; Auto-organisation ; Croissance de nanostructures

1. Introduction

Nucleation and growth of mono-disperse nanostructures is a challenging field both for theoretical modeling and practical applications due to their new magnetic, electric and catalytic properties. Growth of regular islands has been achieved in various systems such as metal aggregates supported on insulator surfaces [1,2], hetero-epitaxial growth of semiconductors including self-assembled quantum dots [3–5], metal on metal systems [6–8] and metal on semiconductors [9]. The use of spontaneously nanostructured substrates as templates for organized growth is a promising way since it allows to grow high density ordered nanostructures over macroscopic scales. This opens up new studies of both individual and collective physical properties by means of usual spatially averaging technics.

The aim of this article is to give an overview of self-organized growth on nanopatterned surfaces. Such epitaxial growth is performed in usual UHV environment. The original point is to take advantage of a spontaneously nanopatterned substrate. Section 2 is devoted to the underlying physics of the nanopatterned substrates. Due to recent development during the last ten years in surface physics, the phenomenon of self-ordering at surfaces is now better understood and leads to a large variety of nanopatterned substrates. Section 3 recalls, in the framework of a mean field model, the concepts of nucleation and growth on surfaces and explains why the occurrence of a surface nanostructuration modifies the epitaxial growth and leads to an organized growth. Then, Section 4 illustrates by experimental examples organized growth on different surfaces. We highlight how it is possible to analyze atomistic processes responsible for the organized growth.

In all this article we restrict the term of self-ordering to equilibrium periodic nanopatterning of surfaces, and self-organization or organization to a wider use, namely the epitaxial growth of atoms on a self-ordered substrate, which is a kinetical growth process.

2. Spontaneously self-ordered nanotemplates

2.1. Nanotemplates overview: surface reconstructions and surface dislocation networks, vicinal surfaces, self-ordered biphases systems

There exist three main classes of surfaces exhibiting spontaneously nano-scale order at thermal equilibrium: reconstructed surfaces and incommensurate adlayers, vicinal surfaces, self-ordered patterns of biphased domains.

(i) *Reconstructed surfaces* are very common in surface science: the reconstruction may appear on clean surface or under adsorption. In some cases, the superstructure mesh is large enough to reach a few nanometers. Without exhaustivity, let us give some examples: for clean surfaces, the most famous examples are the (7×7) superstructure of Si(111) and the superstructure $(22 \times \sqrt{3})$ of Au(111); for incommensurate adlayers the triangular superstructure of Ag on Pt(111) [7], which is shown in Fig. 1(b). The majority of these reconstructed surfaces can be explained in the frame of the Frenkel–Kontorova model [10,11]. The continuous path from Moiré pattern to dislocation network is controlled by the ratio between lateral and normal interactions: in this frame, a Moiré pattern is a network of very wide dislocations. The Au(111) $22 \times \sqrt{3}$ reconstruction [12–14] has been described within the Frenkel–Kontorova frame [10,11,15,16]. It involves a non-uniform compression of the surface atoms along the $[1\bar{1}0]$ direction, with domain walls, also called linear discommensurations, separating surface regions with the correct (fcc) stacking from regions with a faulted (hcp) stacking sequence (cf. Fig. 1(a)). The periodicity between faulted regions is $L_D = 63.6$ Å. The reconstructed layer is 4% denser than the bulk (111) planes. Several systems of metal on metal growth have been found to reconstruct, such as Cu/Ru(0001) [17,18], Ag/Ru(0001) [19] and Cu/Pt(111) [20] (for a review see [21]).

(ii) *Steps on vicinal surfaces* are ordered at a periodicity varying from some tenth of nanometer to some hundred nanometers. This period is fully controlled by the cut angle. The existence of a long range order for temperatures below the roughening transition is due to long range repulsive interactions between steps.

(iii) *Biphased domains* may exhibit self order at a nanometer scale. The two phases can be: chemical species like in the case of O/Cu(110) [22], N/Cu(100) [23] and Pb/Cu(111) [24]; facetted domains of a vicinal surface like in the case of vicinal faces of Au(111) [25,26] and vicinal faces of Si(100) [27,28]; reconstructed domains of different orientation like in the case of Au(111). This so-called 'herring-bone' reconstruction is due to the alternance of $22 \times \sqrt{3}$ reconstructed domains

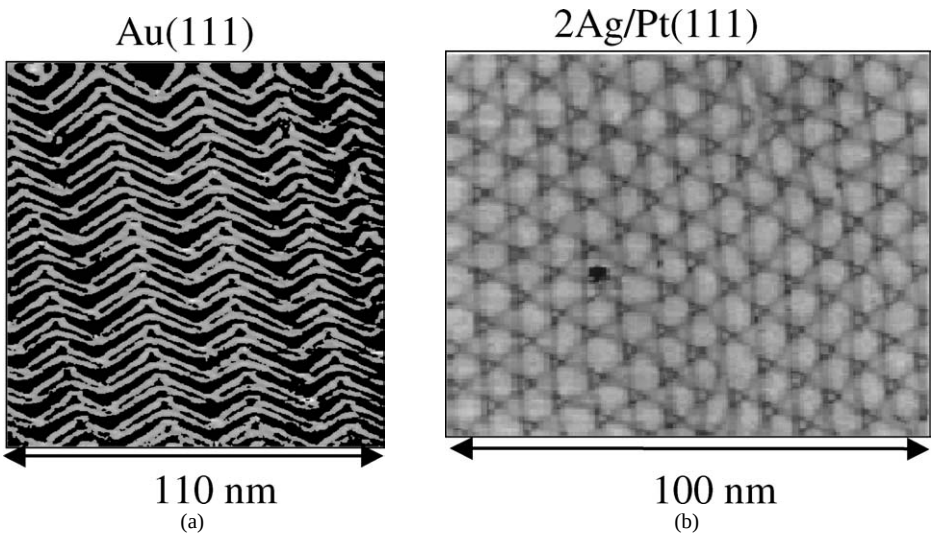

Fig. 1. STM images of: (a) Au(111) reconstruction; (b) a domain wall network formed by the second Ag monolayer on Pt(111) (from [7]).

of two different reconstruction, the periodicity being about 30 nm. In all the cases, the self order of biphased domain needs long range interactions for which elastic interactions are possible candidates.

2.2. Elastic continuum model for long-range ordering at surfaces

Using the formalism of Gibbs for interfacial quantities, a surface stress tensor can be associated to any macroscopic surface phase [29]. In his pioneering paper devoted to facetting, Marchenko [30] pointed out that when two surface phases (different crystallographic faces, dense and dilute adsorbed phases, domains of different in-plane orientation) coexist, the surface stress discontinuities at the phase domain boundaries are equivalent to surface forces (cf. Fig. 2). Due to the elastic response of the substrate to these surface forces, a long-range interaction between boundary parts appears. For periodic striped domains, the energy per unit surface can be written:

$$E = \frac{2E_{\text{micro}}}{L} - \frac{2\alpha_{\text{elas}}(\Delta\sigma)^2}{L}\log\left(\frac{L\sin(\pi\tau)}{2\pi a_c}\right) \tag{1}$$

where L is the period, τ the coverage of one of the two coexisting two-dimensional phases, $\Delta\sigma$ the discontinuity of the surface stress σ_{nn} in the direction n normal to the boundary, α_{elas} a coefficient depending on the bulk elastic constants, a_c a cut-off length and E_{micro} the local energy cost of a boundary.

Several remarks must be made. First, a_c and E_{micro} are not independent parameters, E_{micro} being the part of the boundary energy which cannot be accounted for in the frame of continuous media elasticity and a_c the length beyond which continuous elasticity is valid. Second, using Ostrogradsky theorem, the interaction between lines of force can be transformed in interaction between surface distributions of force dipoles. By the way, the elastic interaction presents a remarkable analogy with other dipolar interactions such as electrostatic or magnetic. The nature – elastic, electrostatic, magnetic – of the dipoles only controls the form and the value of α [31]. Third, in the expression of the energy, the different domains account only by their boundaries. As a consequence, for any domain geometry, the energy E is not changed when the two coexisting phases are mutually exchanged. The symmetry $\tau \to (1-\tau)$ in formula (1) is a consequence of this general rule. Last, for an isotropic medium, the striped geometry is not the only geometry to be considered for the minimization of the interaction energy and the sequence droplet→ striped → inverse droplet is predicted [32] and observed [24] for increasing coverage.

As pointed out by Vanderbilt [33], the difference in work functions associated with two coexisting two-dimensional phases leads to electrostatic dipolar long range interactions. We have already noticed that the dependence of the surface energy on geometry does not allow to distinguish between the elastic and the electrostatic contribution. The a priori estimate of these two effects done by Vanderbilt does not clearly allow such a discrimination. Therefore, to identify the driving force of the self-ordering of crystal surfaces, both measures of surface stress discontinuities and work function differences should be useful. Before discussing the possible ways of measuring surfaces forces, let us remark that in the special case where the self-ordering deals with the orientation of domains (herring-bone pattern of Au(111)), surface stress discontinuity is the only possible driving force since the work function does not depend on domains orientation. Indeed, this model was used in order to explain the

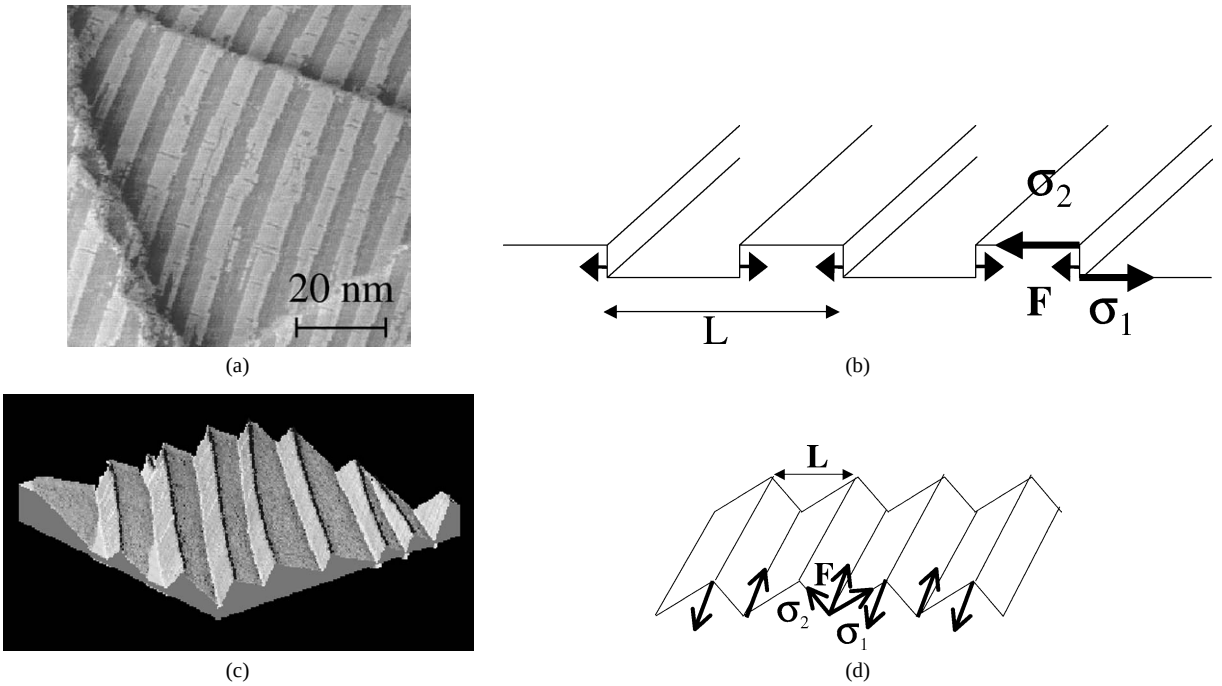

Fig. 2. Self-ordered substrates: (a) STM image of Cu–O striped phase (from [22]); (b) schematic of the Cu–O striped phase showing the forces and the surface stress tensor associated to each chemical phases; (c) 3D STM image of faceted Au(455). The height is not real. The angle between successive facets is 174°; (d) schematic of the 3D hill-and-valley structure.

herring-bone reconstruction of Au(111) [34]. Other successful comparisons between experiments and Marchenko's model have been done in the case of the pioneering system of Cu–O striped domains seen in Fig. 2(a) [22] and in faceted Au(111) vicinal surfaces seen in Fig. 2(c) [25]. In the order between steps of unfaceted vicinal surfaces, long range interactions play a very similar role. Elastic interactions are in this case due to force dipoles at the steps [35]. Therefore, it clearly appears a need for force determinations in self-ordered systems and vicinal faces.

2.3. Surface forces measurements

The standard way to measure surface stress is the cantilever bending method [36]. In this method, the bending of a thin crystal is followed during the deposition of an adsorbate on one side of the crystalline slice. Several methods have been developed to measure the crystal bending (capacitance measurements [37], laser beam deflection [38], ...). They allow to measure differences in surface stress of the order of some $\mathrm{N\,m^{-1}}$ which is a typical value for the adsorption of a monolayer on a metallic substrate. To our knowledge, none of these macroscopic methods has been applied to self-ordered systems. The two methods which have been used to measure surface stress difference in self-ordered systems – the grazing incidence x-ray diffraction (GIXD) [39] the Rutherford backscattering spectrometry (RBS) in channelling geometry [40] – make use of the atomic displacements appearing in the vicinity of a surface stress discontinuity. For a thick crystal, the non-gliding condition implies that the surface strain tensor has components parallel to the surface which are zero on average [29]. As a consequence, the displacements parallel to the surface are zero for a uniform surface. Therefore, the only source of parallel deformations and displacements are the surface stress inhomogeneities, i.e., the surface stress discontinuities appearing at the phase domain boundaries. To measure the corresponding forces, two ingredients are needed: a simplified model for the force distribution and a theoretical frame to deduce the atomic displacements from the force distribution. Let us illustrate the two methods in the case of the self-ordered system N/Cu(100). For coverages less than 0.85 monolayer, chemisorbed nitrogen organizes in square patches of size 5.2 nm. For coverages between 0.4 and 0.85, these patches are organized in two ways (Fig. 3): first, the patches formed regular rows with an intra-row period constant and equal to 5.4 nm; second, the rows are periodically spaced with an inter-row period decreasing with coverage. These two periodicities lead to a rectangular self-ordering. At coverage 0.85, the inter-row period is equal to the intra-row period leading to a square self-ordering [23,41,42]. In a grazing incidence x-ray diffraction experiment, the self-ordering leads to satellite diffraction rods around each crystal truncation rod [39]. Fig. 4 displays the structure factors of such rods for different values of the momentum transfer perpendicular to the surface. The main features of this figure are the

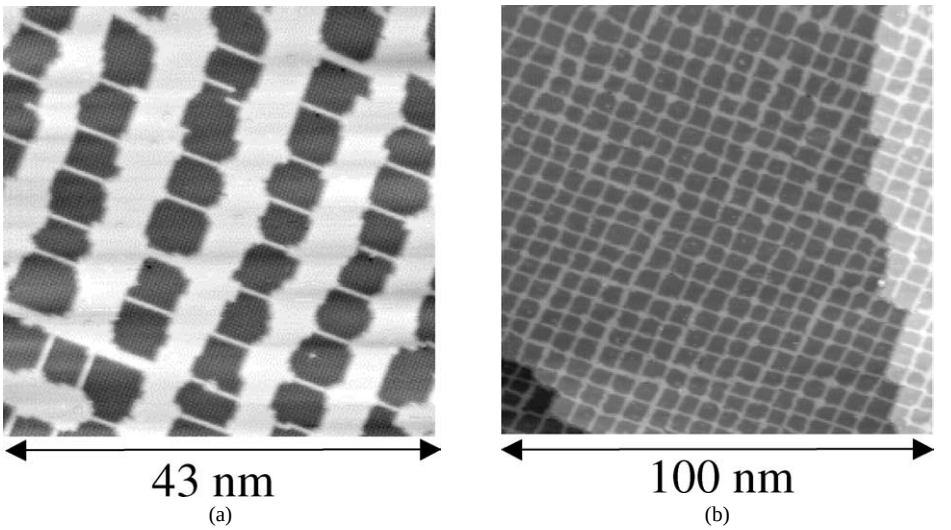

Fig. 3. N/Cu(100) STM images: (a) 43 nm × 43 nm area showing rows of nitrogen square islands and corresponding to 0.6 nitrogen coverage; (b) 100 nm × 100 nm area for 0.9 nitrogen coverage showing the 2D square lattice of nitrogen islands.

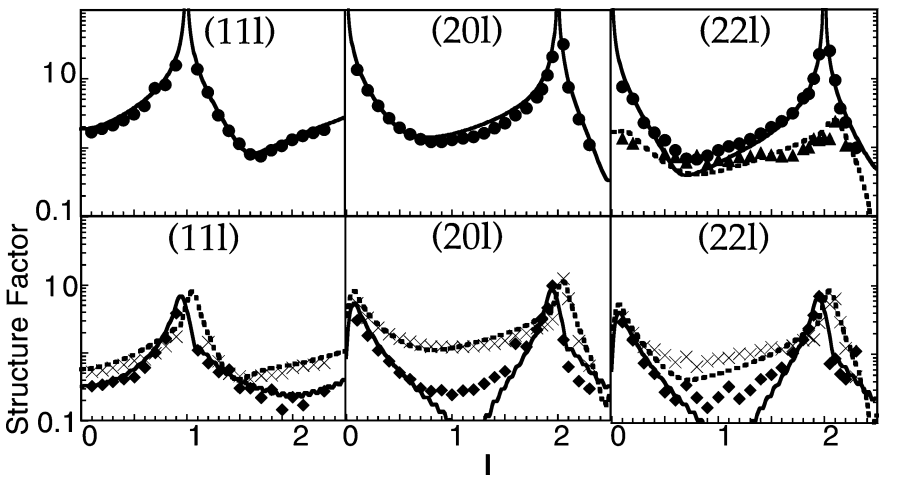

Fig. 4. Experimental and calculated structure factors. Symbols correspond to experimental results and lines to best fit with displacements generated by surface forces of 1 N m^{-1}. Bulk (h,k,l) CTR: ● and full line, $(h+\delta q,k,l)$ satellite: ◆ and full line, $(h-\delta q,k,l)$ satellite: × and dotted line, $(h-\delta q,k-\delta q,l)$ satellite: ▲ and dotted line. $\delta q = 0.071$.

narrow maxima of the structure factors near the Bragg conditions of the Cu substrate. Such features indicate that the diffracting periodic object has as main spatial period in the direction perpendicular to the surface, the interplanar distance of the bulk Cu crystal. This diffracting periodic object consists of the Cu crystal periodically strained by the elastic forces associated with the patches. Fig. 5 displays the corresponding atomic displacements. The chosen force distribution corresponds to punctual forces parallel to the surface applied on the patch boundaries as proposed in Marchenko's model. In this first study, the displacements were calculated with two methods: isotropic linear elastic theory and quenched molecular dynamics using RGL potentials. The fit of the experimental structure factors allows to determine quantitatively the force value, 1 N m^{-1}. The quality of the fit – reliability factor equal to 0.06 – clearly shows that the quite simple force distribution proposed by Marchenko accounts for these experimental results. Rutherford backscattering experiments performed in channelling geometry on the same system show that the same displacement field accounts perfectly well for the dependence of the channelling yield with the $^4He^+$ energy [40]. The GIXD technique has been applied to the self-ordered system O/Cu(110) [43]. It can be extended to the measurements of force dipoles appearing at the steps of vicinal faces. Such measurements have been performed on Pt(977) [44], Cu(322) [45], Au(332) [46]. For both the self-ordered systems and the vicinal faces, the elastic interaction between borders or steps has been

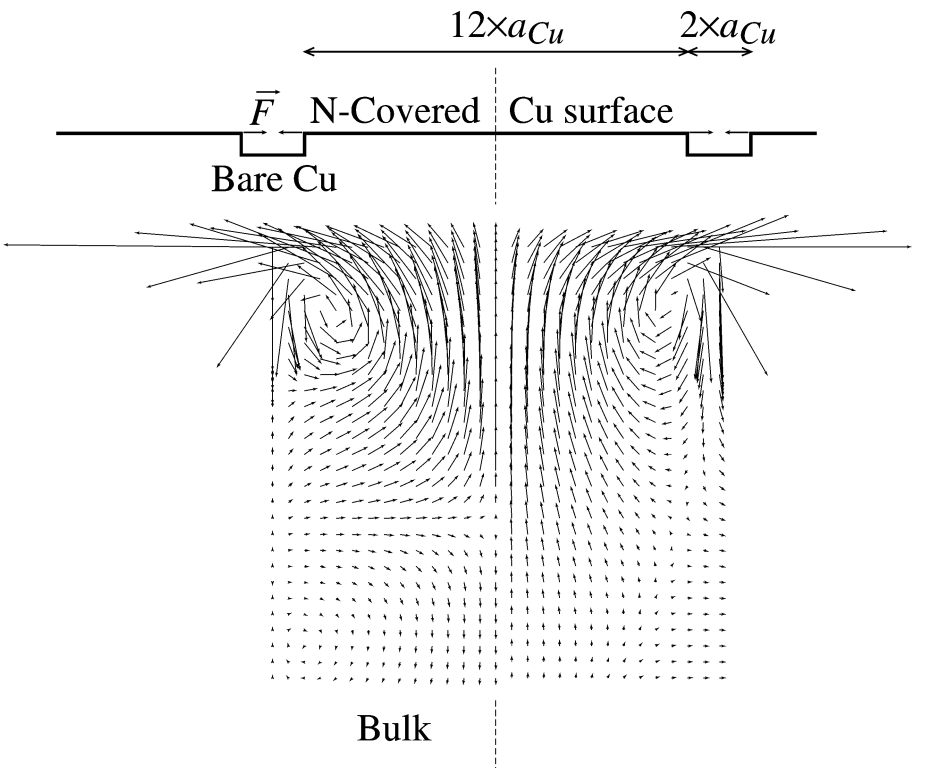

Fig. 5. Transverse section of the atomic relaxations of two consecutive (100) planes. The relaxations are magnified by a factor 50. The dashed line indicates the centre of a domain and the section is perpendicular to a line of domains. Left: relaxations computed by molecular dynamics with surface forces $F = 1\ \mathrm{N\,m^{-1}}$. Right: relaxations calculated in the frame of the linear elasticity with surface forces $F = 1.2\ \mathrm{N\,m^{-1}}$.

found to be at least one order of magnitude greater than the electrostatic interaction. Therefore, our results clearly show that the elastic interaction is the driving force of the order at nanoscale for the metallic systems.

3. Principles for epitaxial organized nucleation and growth

The main principle of self-organization is to use nanopatterned surfaces as templates. Such surfaces display preferential sites and when atoms are deposited from thermal evaporation onto these surfaces, atoms aggregate and replicate the patterned substrate. We recall briefly the random nucleation and growth phenomena and the relevant energetic parameters. Then, we introduce new parameters in order to take into account the periodic nanopattern of the substrate.

3.1. Homogeneous growth

Nucleation and growth of islands on surfaces has been extensively studied for many years and is reviewed in articles or books [21,47]. Atoms are deposited from a vapor pressure onto a surface such as in the common case of solid on solid model. In the case of adatoms moving on a homogeneous substrate (what we call homogeneous growth), the process is well described by mean field theory and is essentially determined by atomistic parameters for surface diffusion and binding energies of adatoms to clusters. Values for these parameters may be determined by comparing scaling predictions with suitable experimental measurements [48]. One usually distinguishes three regimes with increasing coverage of deposited atoms: (i) the nucleation regime where the density of stable islands is increased; (ii) the growth regime where the density is almost constant but the size of islands increases; (iii) the coalescence regime where the density of islands decreases since neighboring islands start to coalesce. The maximum cluster density versus the temperature can be determined from variable temperature STM experiments. In the regime of complete condensation which is relevant for this paper, re-evaporation of adatoms from the substrate into the vapor is absent. The maximum cluster density n_c is given by

$$n_c = \eta (D_0/F)^{-1/3} \exp(E_{\mathrm{diff}}/3k_B T) \tag{2}$$

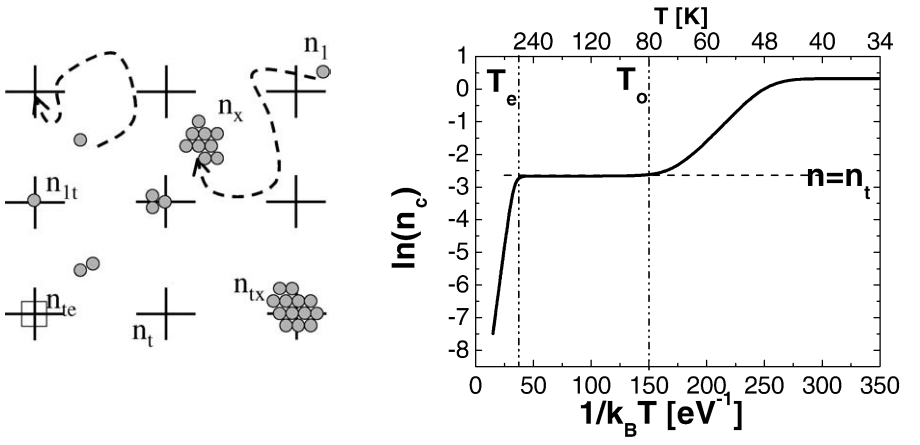

Fig. 6. Mean field model with periodic traps of density n_t. (a) Model for nucleation at periodic traps, which can be occupied by adatoms, density n_{1t}, clusters of size x, density n_{xt}, or can be empty, n_{te}. One has to take also into account adatoms, density n_1, clusters, density n_x such as in the mean field model without traps. (b) Numerical calculation of the mean field model taking into account traps on the surface. It gives the Arrhenius plot of the critical cluster density n_c. The trap energy E_t is 0.7 eV, and the trap density n_t corresponds to the value of the plateau, ranging from T_e to T_o.

where η is a prefactor related to capture numbers, F is the deposition rate (flux), D_0 is the diffusion prefactor, and E_{diff} is the diffusion energy. This expression is valid in the case of stable dimers on the surface i.e. critical cluster size $i = 1$ (i is defined as the size of the biggest unstable cluster). In the case of $i \geqslant 2$, Eq. (2) has to be modified and involves the binding energy to the critical cluster. In the simple $i = 1$ regime, it is worth to notice that the slope of n_c versus T in an Arrhenius plot gives E_{diff}. At higher temperature, the critical nucleus size increases and this leads to a higher slope. Such behavior is also found by using Kinetic Monte-Carlo (KMC) simulations. The advantage of a KMC simulation is that it goes beyond the mean field approximation which is known, for example, to overestimate the islands density. Island shapes, lattice geometry, islands spacings and sizes are also not exactly reproduced in the mean field approximation [21].

3.2. Heterogeneous growth

What happens when the atomic sites on the substrate are not all equivalent? Some sites can act, for example, as preferential nucleation sites. These sites can be described in a mean field model as traps for adatoms [49,50]. Such a model had some success in the past by reproducing the nucleation and growth on surfaces with point defects [1,2]. We show here how it can be applied nicely to the growth on self-ordered surfaces [51]. A schematic of the various events considered in this model and a typical theoretical curve of the critical cluster density versus temperature are shown in Fig. 6 [47,52].

For the lowest temperature, no variation is found: the clusters density is constant with temperature. This corresponds to a low diffusion regime called ‘post-nucleation’ [21] when adatoms hardly diffuse on the surface and are stable. Between 45 K and 80 K, a linear decrease of the cluster density with temperature in an Arrhenius plot is found. At such low temperatures, the adatoms mean free path on the surface is lower than the mean distance between traps. This regime is identical to the homogeneous growth and the slope of the Arrhenius plot is E_{diff}.

Above the temperature threshold T_o, the system displays the organized growth regime. The maximum cluster density is constant, equal to the density of traps. T_o is the temperature at which the adatoms mean free path determined by Eq. (2) is equal to the distance between traps. As a consequence, the parameters which determine T_o are E_{diff} and the traps density n_t.

The organized growth occurs as long as the typical energies of the trapping mechanisms are sufficient to stabilize adatoms in the traps. We call T_e the highest temperature for which an organized growth is observed. The crucial parameter, which determines T_e, is the trap energy E_t. Above T_e, the critical island density decreases dramatically with temperature. The slope is higher than a simple homogeneous growth regime. Such a high value is mainly due to the long time spent by adatoms in traps. The effect of traps is then to reduce the effective diffusion of adatoms [52].

Eventually, the mean field calculations including traps give a qualitative understanding of the organized growth. Rapid adatom diffusion and strong trapping are the main ingredients to get an organized growth over a large temperature range.

In this regime of organized growth, the nucleation sites are periodically arranged. Therefore the capture areas are similar and this leads to regular islands, with a size distribution much narrower than on a homogeneous substrate. Binomial size distribution

has been reported in the regime of ordered growth [7]. The size distribution phenomenon is difficult to address in the framework of a mean field theory and needs KMC simulations for an accurate study [51].

4. Nucleation and growth of ordered nanostructures: examples and atomic processes

This part of the article is devoted to applications of self-ordered substrates in the field of epitaxial growth. Three kinds of substrates are considered here. We start with close-packed surfaces showing either long period reconstruction such as stress relief patterns, or self-ordered domains induced by an adsorbate. Then, vicinal surfaces are well known substrates where it is possible to growth one-dimensional nanostructures along steps. Eventually, more complex substrates are proposed which are a combination between the stress relief patterned found on close-packed surfaces and the vicinality of surfaces.

4.1. Self-organized growth on close-packed surfaces

Nanopatterned substrates can be used as templates for guiding the growth of adatoms. This is first illustrated with the substrate N–Cu(100) almost completely covered with nitrogen (as seen in Fig. 3(b)). When gold atoms are deposited onto this surface with submonolayer coverages, nitrogen areas act as a mask for the growth of gold atoms. The gold islands nucleate on bare copper areas only and this leads to a square lattice of gold islands (cf. Fig. 7). The distance between two islands is about 5 nm. The gold islands display a square shape and they are not connected with each other [53]. The complex patterns of the copper substrate covered with nitrogen open up a wide variety of patterns. Several other metals (Fe [54,55], Co [56–58], Ni [59] and Ag [60,61]) have been deposited on such substrates.

Another class of systems are surface dislocations networks. It was early recognized that the Au(111) herring-bone reconstruction leads to organized growth. It has been used with several kind of atoms: Ni [6,62], Fe [63,64], Co [63,65,66], Pd [67], Mn [68] and Rh [68]. The herring-bone structure gives rise to a periodic array of surface dislocations located at the elbows. These surface dislocation arrays act as preferential nucleation sites via a place exchange mechanism occurring mainly at room temperature. This mechanism has been demonstrated for Ni [62] and Co [69] (cf. Fig. 8(a)).

Similar surface dislocations networks can be obtained in a more general way in the hetero-epitaxial growth of metals on metals. However, only a very few of them have been widely used for self-organized growth. Several examples have been demonstrated by Brune and coworkers [7]. The deposition of silver atoms on a template made of 2 monolayers of silver deposited on Pt(111) was able to reproduce the initial nanopatterning of the substrate (cf. Fig. 8(b)). The same authors also used the system of Fe/Cu/Pt(111).

Eventually, all these examples show that it is indeed possible to use the nanopatterning of substrates in order to grow nanostructures very regular in sizes and spacings. In this way very high density of nanostructures is achieved. However, it depends on a crucial parameter which is the temperature of the substrate for the deposition. Several mechanisms have been reviewed. However, one drawback of the organized growth on close packed surface is the occurrence of defects, such as steps which can break either the phase coherence of the nanostructure lattice, or even the lattice symmetry. Therefore the ordering remains very local on such flat surfaces. In order to improve this growth in achieving long range ordered organized growth, the ideal substrates are the vicinal surfaces.

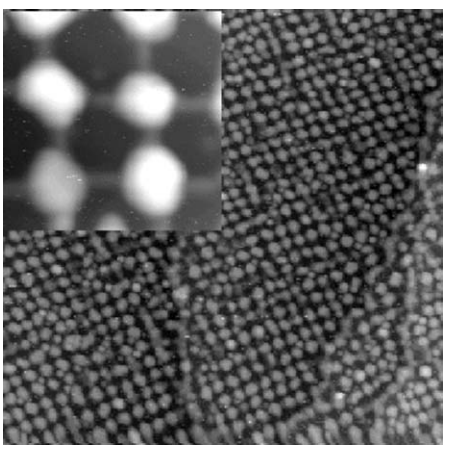

Fig. 7. STM image of area 150 nm × 150 nm showing gold islands arranged in a square lattice on the N/Cu(100) substrate after a deposit of 0.8 ML at room temperature. The inset is a zoom into four gold nanoislands separated by 5 nm.

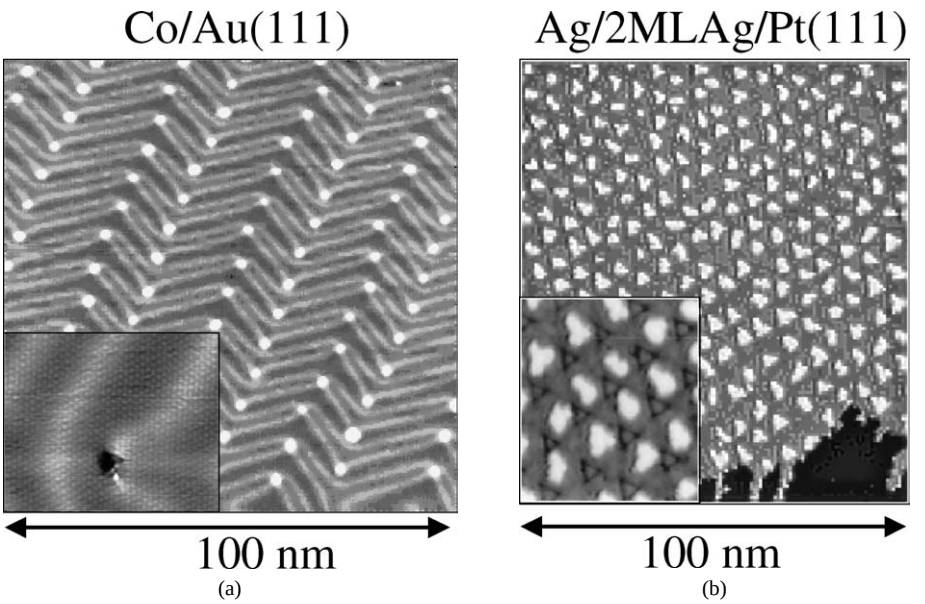

Fig. 8. (a) 0.1 ML cobalt deposited on a Au(111) surface. The inset shows atomic resolution of 0.005 ML of cobalt deposition on Au(111) at room temperature. Inserted Co atoms appear 0.04 nm darker than the gold surface; (b) Ag nucleation on the network shown in Fig. 1(b). Deposition at 110 K yields an island superlattice with exactly one island per superstructure unit cell (coverage of 0.1 ML) (from [21]).

4.2. One-dimensional long range organized growth on vicinal surfaces

Vicinal surfaces, i.e. surfaces slightly misoriented with respect to a close-packed surface, have attracted a wide interest in many areas, such as catalysis and nanostructure growth. Since they display a well-controlled number of steps, they are model systems for studying the interaction between steps and surface phenomena such as reconstruction, adsorption, and diffusion. Nowadays, they serve as templates for building one-dimensional periodic nanostructures of regular sizes [70–72]. Indeed the step sites provide preferential nucleation sites for the growth of adatoms. Large wires have been grown along steps (see [71]). Recently, cobalt wires down to atomic width have been successfully grown on a Pt(997) surface [73] and their magnetic properties were also investigated [74,75].

4.3. Two-dimensional long range organized growth: combining stress relief patterned and vicinal surfaces

In Section 4.1, we have seen that organized islands can be grown on strain relief patterned close-packed surfaces. For optimized growth parameters such as temperature, these islands are highly regular in sizes and spacings. The prominent result is the very narrow islands size distribution, comparable to the metal nanoparticule colloids usually obtained by wet chemistry (i.e. methods based on chemical reactions in solution) see references in [76]) or in the article of Bruno Chaudret in this issue. However, the organization of islands on close-packed surfaces remains very local: there is order all over, but no phase coherence over more than the terrace width. In Section 4.2, long range order was achieved by using vicinal substrates. By combining both vicinal surfaces and stress relief patterns or reconstruction, it is possible to achieve the growth of 2D long range ordered islands. This was first achieved in the system Co on Au(111) vicinal surfaces [77,69], in particular using the model Au(788) surface. The Au(788) substrate is a stable, vicinal surface misoriented by 3.5° with respect to the (111) plane toward the $[-211]$ azimuth. The surface displays a highly regular succession of mono-atomic steps and 3.8 nm wide terraces. Due to the $22 \times \sqrt{3}$ reconstruction of the Au(111) plane, Au(788) is also reconstructed in the direction perpendicular to the steps (7.2 nm periodicity) (cf. inset in Fig. 9(a)). It is worth noting the importance of the step direction. Indeed, due to the interaction of the discommensuration line with the step, only vicinal surfaces with {111}-steps (toward the $[-211]$ azimuth) display such a pattern [77]. For other step directions, different patterns can be expected (for example, on the Au(12,11,11) a more complex pattern has been found [26]). The Au(788) surface can be used as a template for the growth of cobalt nanodots since the crossing of a discommensuration line and a step edge acts as a preferred nucleation site as seen in Fig. 9 [69,78,79,77].

In order to understand microscopic mechanisms responsible for this growth, we have performed variable temperature scanning tunneling experiments (VT-STM) and multi-scaled simulations. Characteristic VT-STM images are displayed in Fig. 10(a). The organized growth is not seen at the lowest and at the highest temperatures. It occurs only in a certain temperature range.

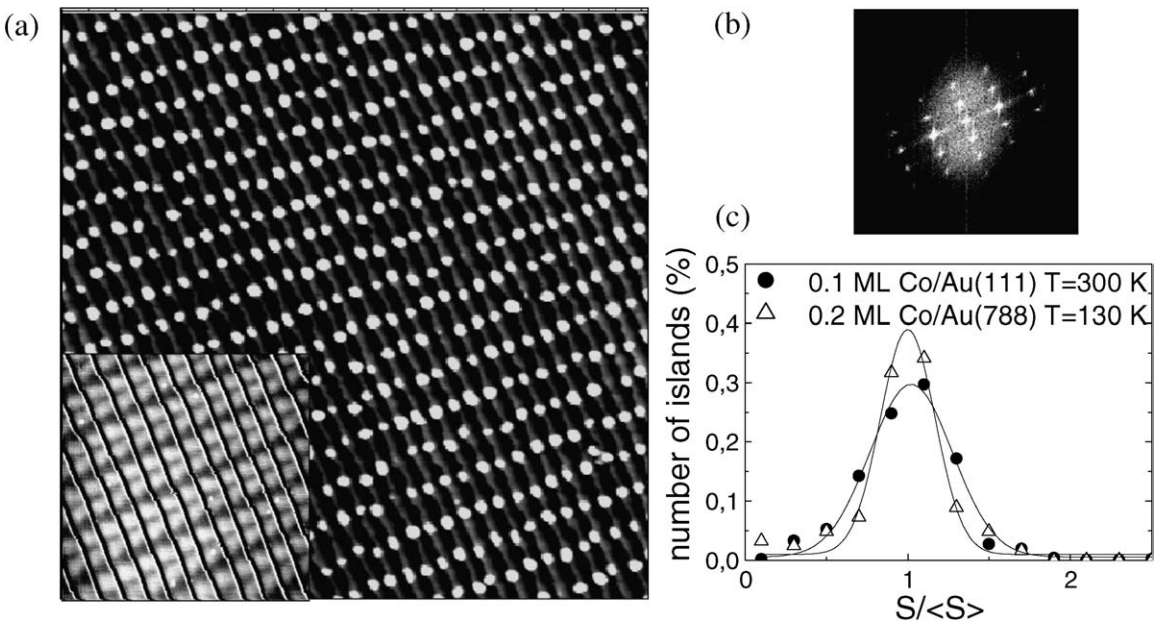

Fig. 9. (a) Large scale STM image of 0.2 ML Co deposition on Au(788) at 130 K subsequent annealing to 300 K, area 100 nm × 100 nm. The inset shows the discommensuration lines running perpendicular to the step edges (the image area is 45 nm × 45 nm). The corrugation due to the terrace levels has been substracted in order to enhance the reconstruction lines. (b) Fast Fourier transform of the STM image; (c) normalized islands distributions of 0.2 ML Co on Au(788) at 130 K and 0.1 ML of Co on Au(111) at room temperature. The mean island size $\langle S \rangle$ is 5 and 10 nm^2, respectively for Co on Au(788) and on Au(111).

Analysis of VT-STM images allows to plot exactly the curve of the maximum cluster density versus temperature (cf. Fig. 10(b)). The energetics of the atomistic growth is contained within this curve, as it has been explained in Section 3.2. Images clearly show that there are two preferred sites at each lattice point of the 2D structuration of the substrate (cf. Fig. 10(a)). According to this observation, the plateau of the curve appears at this sites density. In this example, the plateau is particularly large ranging from 60 K to 300 K, compared to what has been obtained on previous metal on metal system [7]. The fit of this experimental curve with the mean field approximation is good with a trap energy $E_t = 0.7$ eV. Now the question is how we can understand this value. What mechanism can be responsible for such a value? In this system two microscopic mechanisms can be invoked: either preferred adsorption since such preferred site was foreseen in MD calculations [80], or place exchange mechanism since we do observe such a site at room temperature [69]. On the one hand, the energetics of the preferred adsorption site has been calculated by MD, and the value is much smaller than $E_t = 0.7$ eV. Therefore this mechanism alone cannot explain the extensive plateau. On the other hand, performing KMC simulations with the place exchange mechanism only do not lead to any plateau. Thus the conclusion is that none of these mechanism alone is able to reproduce satisfactorily the curve of the critical cluster density versus temperature. However, we were able to reproduce very well this curve with realistic energetic values only by taking into account both mechanisms (cf. Fig. 10).

This example shows that the description using mean field calculations including traps is only qualitative. Each system will display different microscopic mechanisms for explaining the trap sites: preferred adsorption, place exchange mechanism, repulsive energy barrier. Each mechanism is associated to exact energetic parameters which can be determined by calculations (ab-initio methods or Quenched Molecular Dynamics (QMD)). Determination of energetic parameters and KMC simulations are very powerful in understanding the real atomistic mechanisms associated which each system. The other example that has been also studied in detail is the example of Ag on Pt [21]. Eventually KMC simulations allows also to understand the size distribution of islands [51].

5. Conclusion

As a summary, we have shown how self-ordering at surfaces can be used for growing nanostructures regular in size and spacing. Due to progress in surface science, there exists a large variety of surfaces which display nanopatterning over large areas. In self-ordered surfaces, bulk elastic relaxations due to surface stress discontinuities is the driving force for stabilizing

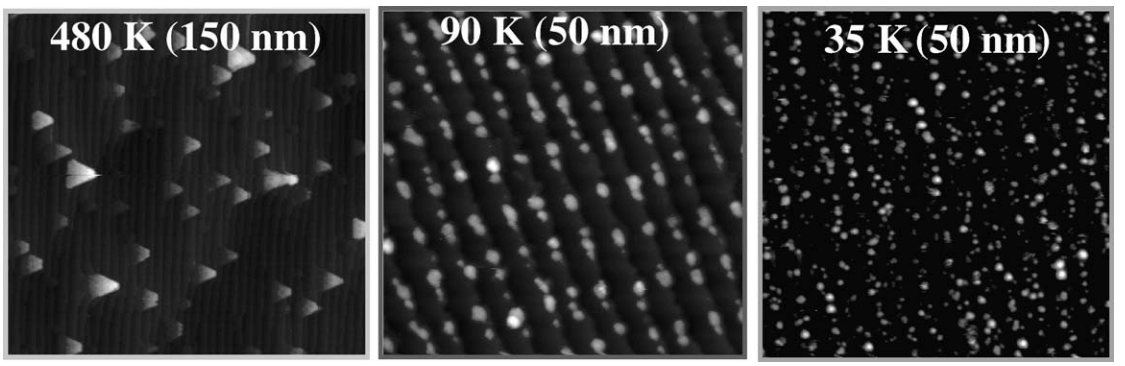

(a)

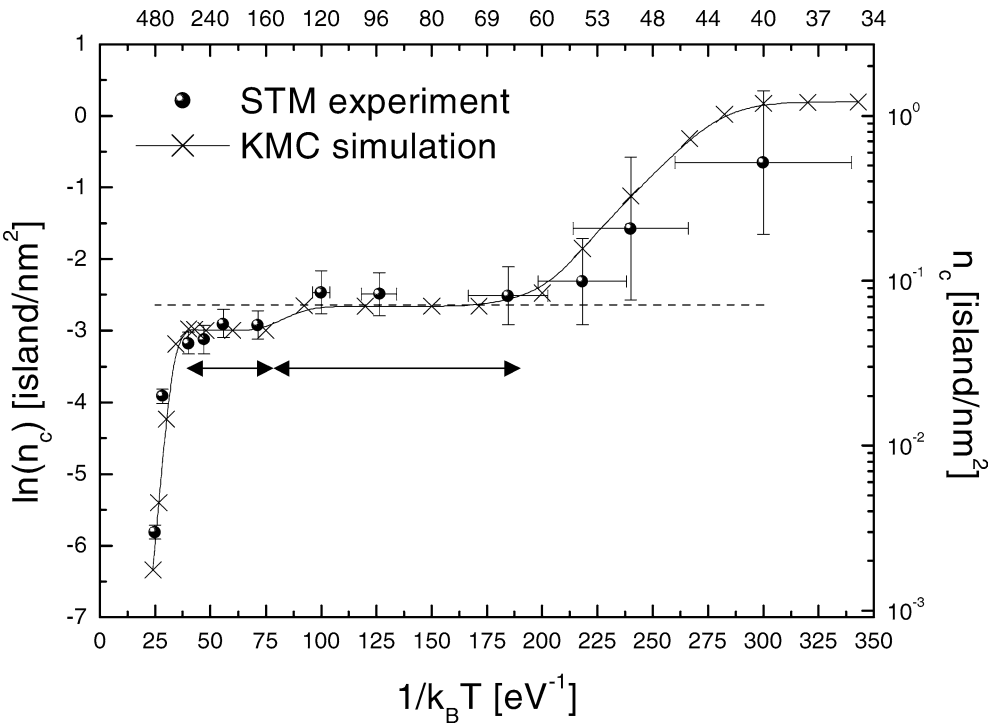

(b)

Fig. 10. (a) STM images of cobalt deposited on Au(788) at different temperatures. From left to right the temperature is 480 K, 95 K and 35 K. Except for 480 K the STM images are obtained at the deposition temperature. Area sizes are respectively 150 nm × 150 nm, and 50 nm × 50 nm for last ones. Coverage of cobalt is respectively 0.4 ML, 0.3 ML, and 0.6 ML; (b) KMC simulation of the growth of Co nanodots on Au(788). A good fit to experimental data for the critical cluster density versus temperature is obtained with the model combining both the adsorption and place exchange mechanisms in the preferred sites. The left double arrow points out the 160 K-room temperature range where place exchange mechanism is efficient in addition to preferred adsorption, whereas the adsorption alone is responsible for the organized growth at the 65 K–160 K range indicated by the right double arrow.

periodic domain formation. Such periodic domain formation includes faceted surfaces, dislocations networks, and metal surfaces covered by an adsorbate. Recent GIXD experiments have been able to measure directly the bulk displacements due to the elastic forces. Then, these self-ordered surfaces can be used as templates for organized growth. This allows to elaborate very high density of regular nanostructures. The organized growth appears usually within a temperature range for the temperature deposition. This is due to kinetically limited growth. We have shown that a simple Rate Equation model modified in order to account for the preferred nucleation sites is able to qualitatively reproduce the epitaxial organized growth behavior. However microscopic mechanisms are complex and are determined only by extensive comparison between experiments and calculation. Eventually, by using both vicinal surfaces and strain relief patterns, one can improve the 2D long range organized growth of

nanostructures. This might be of crucial importance for determining physical properties of nanoparticles, with respect to their shape and interactions.

Acknowledgements

We are very grateful to Harald Brune for providing us with Figs. 1(b), and 8(b) and Peter Zeppenfeld for Fig. 2(a).

References

[1] G. Haas, A. Menck, H. Brune, J. Barth, J. Venables, K. Kern, Nucleation and growth of supported clusters at defect sites: Pd/MgO(001), Phys. Rev. B 61 (2000) 11105.
[2] K. Heim, S. Coyle, G. Hembree, J. Venables, Growth of nanometer-size metallic particles on CaF_2(111), J. Appl. Phys. 80 (1996) 1161.
[3] G. Springholz, V. Holy, M. Pinczolits, G. Bauer, Self-organized growth of three-dimensional quantum dot crystals with fcc-like stacking and a tunable lattice constant, Science 282 (1998) 734.
[4] J. Tersoff, C. Teichert, M. Lagally, Self-organization in growth of quantum dot supperlattices, Phys. Rev. Lett. 76 (1996) 1675.
[5] Q. Xie, A. Madhukar, P. Chen, N. Kobayashi, Vertically self-organized InAs quantum box islands on GaAs(100), Phys. Rev. Lett. 75 (1995) 2542.
[6] D. Chambliss, R. Wilson, S. Chiang, Nucleation of ordered Ni island arrays on Au(111) by surface-lattice dislocations, Phys. Rev. Lett. 66 (1991) 1721.
[7] H. Brune, M. Giovannini, K. Bromann, K. Kern, Self-organized growth of nanostructure arrays on strain-relief patterns, Nature 394 (1998) 451.
[8] O. Fruchart, M. Klaua, J. Barthel, J. Kirschner, Self-organized growth of nanosized vertical magnetic Co pillars on Au(111), Phys. Rev. Lett. 83 (1999) 2769.
[9] C. Teichert, Self-organization of nanostructures in semiconductor heteroepitaxy, Phys. Rep. 365 (2002) 335–432.
[10] Y. Frenkel, T. Kontorova, On the theory of plastic deformation and twinning, Zh. Eksp. Teor. Fiz. 8 (1938) 1340.
[11] F. Frank, J. Van der Merwe, One dimensional dislocations, Proc. R. Soc. London Ser. A 198 (1949) 205.
[12] U. Harten, A. Lahee, J. Toennis, C. Wöll, Observation of a soliton reconstruction of Au(111) by high-resolution helium-atom diffraction, Phys. Rev. Lett. 54 (1985) 2619.
[13] C. Wöll, S. Chiang, R. Wilson, P. Lippel, Determination of atom positions at stacking-fault dislocations on Au(111) by scanning tunneling microscopy, Phys. Rev. B 39 (1989) 7988.
[14] J. Barth, H. Brune, G. Ertl, R. Behm, Scanning tunneling microscopy observations on the reconstructed Au(111) surface: atomic structure, long-range superstructure, rotational domains and surface defects, Phys. Rev. B 42 (1990) 9307.
[15] M. El-Batanouny, S. Burdick, K. Martini, P. Stancioff, Double sine Gordon solitons: a model for misfit dislocations on the Au(111) reconstructed surface, Phys. Rev. Lett. 58 (1987) 2762.
[16] R. Ravelo, M. El-Batanouny, Molecular-dynamics study of the reconstructed Au(111) surface: low temperature, Phys. Rev. B 40 (1989) 9574.
[17] C. Günther, J. Vrijmoeth, R. Hwang, R. Behm, Strain relaxation in hexagonally close-packed metal–metal interfaces, Phys. Rev. Lett. 74 (1995) 754.
[18] H. Zajonz, D. Gibbs, A. Baddorf, V. Jahns, D. Zehner, Structure and growth of strained Cu films on Ru(0001), Surf. Sci. 447 (2000) L141–L146.
[19] R. Hwang, J. Hamilton, J. Stevens, S. Foiles, Near-surface buckling in strained metal overlayer systems, Phys. Rev. Lett. 75 (1995) 4242.
[20] B. Holst, M. Nohlen, K. Wandelt, W. Allison, Observation of an adlayer-driven substrate reconstruction in Cu–Pt(111), Phys. Rev. B 58 (1998) R10195.
[21] H. Brune, Microscopic view of epitaxial metal growth: nucleation and aggregation, Surf. Sci. Rep. 31 (1998) 121.
[22] K. Kern, H. Niehus, A. Schatz, P. Zeppenfeld, J. Goerge, G. Comsa, Long-range spatial self-organization in the adsorbate-induced restructuring of surfaces: Cu{110}–(2×1)O, Phys. Rev. Lett. 67 (1991) 855.
[23] F. Leibsle, S.S. Dhesi, S. Barrett, A. Robinson, STM observations of Cu(100) $c(2 \times 2)$N surfaces: evidence for attractive interactions and an incommensurate $c(2 \times 2)$ structure, Surf. Sci. 317 (1994) 309.
[24] R. Plass, J. Last, N. Bartelt, G. Kellogg, Self-assembled domain patterns, Nature 412 (2001) 1975.
[25] V. Repain, J. Berroir, B. Croset, S. Rousset, Y. Garreau, V. Etgens, J. Lecoeur, Interplay between atomic and mesoscopic order on gold vicinal surfaces, Phys. Rev. Lett. 84 (2000) 5367.
[26] S. Rousset, V. Repain, G. Baudot, Y. Garreau, J. Lecoeur, Self-ordering of Au(111) vicinal surfaces and application to nanostructure organized growth, J. Phys.: Condens. Matter. 15 (2003) S3363–S3392.
[27] S. Song, S. Mochrie, G. Stephenson, Faceting kinetics of stepped Si(113) surfaces: a time-resolved X-ray scattering study, Phys. Rev. Lett. 74 (1995) 5240.
[28] S. Song, M. Yoon, S. Mochrie, G. Stephenson, S. Milner, Faceting kinetics of stepped Si(113) surfaces: dynamic scaling and nano-scale grooves, Surf. Sci. 372 (1997) 37.
[29] P. Müller, A. Saúl, Elastic effects on surface physics, Surf. Sci. Rep. 54 (2004) 157.

[30] V. Marchenko, Theory of the equilibrium shape of crystals, Sov. Phys. JETP 54 (1981) 605.
[31] M. Seul, D. Andelman, Domain shapes and patterns: the phenomenology of modulated phases, Science 267 (1995) 476.
[32] K. Ng, D. Vanderbilt, Stability of periodic domain structures in a two-dimensional dipolar model, Phys. Rev. B 52 (1995) 2177.
[33] D. Vanderbilt, Phase segregation and work-function variations on metal surfaces: spontaneous formation of periodic domain structures, Surf. Sci. 268 (1992) L300.
[34] S. Narasimhan, D. Vanderbilt, Elastic stress domains and the herringbone reconstruction on Au(111), Phys. Rev. Lett. 69 (1992) 1564.
[35] V. Marchenko, A. Parshin, Elastic properties of crystal surfaces, Sov. Phys. JETP 52 (1980) 129.
[36] H. Ibach, The role of surface stress in reconstruction, epitaxial growth and stabilization of mesoscopic structures, Surf. Sci. Rep. 29 (1997) 193.
[37] R. Abermann, Measurements of the intrinsic stress in thin metal films, Vacuum 41 (1990) 1279.
[38] A. Schell-Sorokin, R. Tromp, Mechanical stresses in (sub)monolayer epitaxial films, Phys. Rev. Lett. 64 (1990) 1039.
[39] B. Croset, Y. Girard, G. Prévot, M. Sotto, Y. Garreau, R. Pinchaux, M. Sauvage-Simkin, Measuring surface stress discontinuities in self-organized systems with X rays, Phys. Rev. Lett. 88 (2002) 56103.
[40] C. Cohen, H. Ellmer, J. Guigner, A. L'Hoir, G. Prévot, D. Schmaus, M. Sotto, Surface relaxation and near-surface atomic displacements in the N/Cu(100) self-ordered system, Surf. Sci. 490 (2001) 336.
[41] M. Sotto, B. Croset, Self-organisation of adsorbed nitrogen on (100) and (410) copper faces: a SPA-LEED study, Surf. Sci. 461 (2000) 78.
[42] H. Ellmer, V. Repain, S. Rousset, B. Croset, M. Sotto, P. Zeppenfeld, Self-ordering in two dimensions: nitrogen adsorption on copper (100) followed by STM at elevated temperature, Surf. Sci. 476 (2001) 95.
[43] G. Prévot, B. Croset, Y. Girard, A. Coati, Y. Garreau, M. Hohage, L.D. Sun, P. Zeppenfeld, Elastic origin of the O/Cu(110) self-ordering evidenced by GIXD, Surf. Sci. 549 (2004) 52.
[44] G. Prévot, P. Steadman, S. Ferrer, Determination of the elastic dipole at the atomic steps of Pt(977) from surface X-ray diffraction, Phys. Rev. B 67 (2003) 245409.
[45] G. Prévot, A. Coati, Y. Garreau, GIXD measurement of the relaxations and elastic step interactions on Cu(211) and Cu(322), Phys. Rev. B 70 (2004) 205406.
[46] G. Prévot, L. Barbier, G. Baudot, Y. Girard, V. Repain, S. Rohart, S. Rousset, unpublished.
[47] J. Venables, Introduction to Surface and Thin Film Processes, Cambridge Univ. Press, Cambridge, 2000.
[48] H. Brune, G. Bales, J. Jacobsen, C. Boragno, K. Kern, Measuring surface diffusion from nucleation island densities, Phys. Rev. B 60 (1999) 5991.
[49] J. Venables, P. Bennett, H. Brune, J. Drucker, J.H. Harding, Selective nucleation and controlled growth: quantum dots on metal, insulator and semiconductor surfaces, Philos. Trans. R. Soc. London Ser. A 361 (2003) 311.
[50] J. Venables, Nucleation growth and pattern formation in heteroepitaxy, Physica A 239 (1997) 35.
[51] S. Rohart, G. Baudot, V. Repain, Y. Girard, S. Rousset, H. Bulou, C. Goyhenex, L. Proville, Atomistic mechanisms for the ordered growth of Co nanodots on Au(788): a comparison between VT-STM experiments and multiscale calculations, Surf. Sci. 559 (2004) 47–62.
[52] S. Rohart, G. Baudot, V. Repain, Y. Girard, S. Rousset, Site selective nucleation on surfaces: the rate equation model compared with VT-STM experiment of Co on Au(788), Proceedings of ICCG-14, J. Cryst. Growth, in press.
[53] H. Ellmer, V. Repain, M. Sotto, S. Rousset, Pre-structured metallic template for the growth of ordered, square-based nanodots, Surf. Sci. 511 (2002) 183.
[54] T. Parker, L. Wilson, N. Condon, F. Leibsle, Epitaxy controlled by self-assembled nanometer-scale structures, Phys. Rev. B 56 (1997) 6458.
[55] S. Ohno, K. Nakatsuji, F. Komori, Growth mechanism of Fe nanoisland array on Cu(100)–c(2×2)N surfaces, Surf. Sci.
[56] S. Silva, S. Jenkins, S. York, F. Leibsle, Fabricating nanometer-scale Co dot and line arrays on Cu(100) surfaces, Appl. Phys. Lett. 76 (2000) 1128.
[57] K. Mukai, Y. Matsumoto, K. Tanaka, F. Komori, Self-organized structure in Co thin film growth on c(2×2)–N–Cu(100) surfaces, Surf. Sci. 450 (2000) 44.
[58] F. Komori, K. Lee, K. Nakatsuji, T. Iimori, Y. Cai, Growth and magnetism of Co nanometer-scale dots squarely arranged on Cu(001)–c(2×2)N surface, Phys. Rev. B 63 (2001) 214420.
[59] Y. Matsumoto, K. Tanaka, Jpn. J. Appl. Phys. 37 (1998) L154.
[60] S. Silva, F. Leibsle, Fabricating nanometer-scale Ag lines and islands on Cu(100) surfaces, Surf. Sci. 440 (1999) L835.
[61] F. Leibsle, Nanostructure fabrication on copper surfaces, Surf. Sci. 514 (2002) 33–40.
[62] J. Meyer, I. Baikie, E. Kopatzki, R. Behm, Preferential island nucleation at the elbows of the Au(111) herringbone reconstruction through place exchange, Surf. Sci. 365 (1996) L647.
[63] B. Voigtländer, G. Meyer, N. Amer, Epitaxial growth of Fe on Au(111): a scanning tunneling microscopy investigation, Surf. Sci. 225 (1991) L529.
[64] J. Stroscio, D. Pierce, R. Dragoset, P. First, Microscopic aspects of the initial growth of metastable fcc iron on Au(111), J. Vac. Sci. Technol. A 10 (1992) 1981.
[65] B. Voigtländer, G. Meyer, N. Amer, Epitaxial growth of thin magnetic cobalt films on Au(111) studied by scanning tunneling microscopy, Phys. Rev. B 44 (1991) 10354.
[66] S. Padovani, F. Scheurer, J. Bucher, Burrowing self-organized cobalt clusters into a gold substrate, Europhys. Lett. 45 (1999) 327.
[67] A. Stephenson, C. Baddeley, M. Tikhov, R. Lambert, Nucleation and growth of catalytically active Pd islands on Au(111)-22$\times\sqrt{3}$ studied by scanning tunneling microscopy, Surf. Sci. 398 (1998) 172.
[68] E. Altman, R. Colton, Growth of Rh on Au(111): surface intermixing of immiscible metals, Surf. Sci. 304 (1994) L400.

[69] V. Repain, G. Baudot, H. Ellmer, S. Rousset, Two-dimensional long-range ordered growth of uniform cobalt nanostructures on a Au(111) vicinal template, Europhys. Lett. 58 (2002) 730.
[70] V. Shchukin, D. Bimberg, Spontaneous ordering of nanostructures on crystal surfaces, Rev. Mod. Phys. 71 (1999) 1125.
[71] F. Himpsel, J. Ortega, G. Mankey, R. Willis, Magnetic nanostructures, Adv. Phys. 47 (1998) 511.
[72] J. Shen, R. Skomski, M. Klaua, J. Jenniches, S. Manoharan, J. Kirschner, Magnetism in one dimension: Fe on Cu(111), Phys. Rev. B 56 (1997) 2340.
[73] P. Gambardella, M. Blanc, L. Bürgi, K. Kuhnke, K. Kern, Co growth on Pt(997): from monatomic chains to monolayer completion, Surf. Sci. 449 (2000) 93.
[74] P. Gambardella, A. Dallmeyer, K. Maiti, M. Malagoli, W. Eberhardt, K. Kern, C. Carbone, Ferromagnetism in one-dimensional monatomic metal chains, Nature 416 (2002) 301.
[75] P. Gambardella, S. Rusponi, M. Veronese, S. Dhesi, C. Grazioli, A. Dallmeyer, I. Cabria, R. Zeller, P. Dederichs, K. Kern, C. Carbone, H. Brune, Giant magnetic anisotropy of single cobalt atoms and nanoparticules, Science 300 (2003) 1130.
[76] L. Liz-Marzan, Nanometals: formation and color, Materialstoday 7 (2004) 26.
[77] V. Repain, J. Berroir, S. Rousset, J. Lecoeur, Growth of self-organized cobalt nanostructures on Au(111) vicinal surfaces, Surf. Sci. 447 (2000) L152.
[78] V. Repain, G. Baudot, H. Ellmer, S. Rousset, Ordered growth of cobalt nanostructures on Au(111) vicinal surfaces: nucleation mechanism and temperature behavior, Mat. Sci. Engin. B 96 (2002) 178.
[79] G. Baudot, S. Rohart, V. Repain, H. Ellmer, Y. Girard, S. Rousset, Temperature dependence of ordered cobalt nanodots growth on Au(788), Appl. Surf. Sci. 212–213 (2003) 360.
[80] C. Goyhenex, H. Bulou, Theoretical insight in the energetics of Co adsorption on a reconstructed Au(111) substrate, Phys. Rev. B 63 (2001) 235404.